Anatomical Variations of Coeliac Axis and Common Hepatic Artery- Systematic Analysis of Multi detector Computed Tomography Images

Authors
Dr Bindu.R.Kumar[1], Dr Umesan K G[2]
[1]Assistant Professor, Dept of Radiodiagnosis, Government Medical College, Thiruvananthapuram
Email: *bindupai@hotmail.com*
[2]Assistant Professor, Dept of Anatomy, Govt. Medical College, Thiruvananthapuram
Corresponding Author
Dr Umesan K G
Email: *umesankg@yahoo.com*

Abstract
Purpose: *The study was conducted to identify and evaluate the spectrum of anatomical variations of the coeliac axis (CA) and common hepatic artery(CHA) seen in multi detector computed tomography (MDCT) images .*
Materials and Methods: *The pattern of origin, course and branching of coeliac axis and common hepatic artery were evaluated in CT images of patients in Dept of Radiodiagnosis, Government Medical College, Trivandrum. A pre described nomenclature system is used for the systematic description of coeliac axis and common hepatic artery variations.CHA was defined as an arterial trunk containing at least one segmental hepaticartery and the gastroduodenal artery.*
After assessing the coeliac axis anatomy the branching pattern of the downstream hepatic arteries including their origin site, anatomic course specifically of the common hepatic, left and right hepatic arteries and the gastroduodenal artery was studied.
Results: *A total of 149 out of 150 cases had a normal celiac axis anatomy which appeared as a hepatogastrosplenic trunk and SMA originating separately from the aorta (HSpM+SM). Variant identified was a hepatogastric trunk with splenomesenteric trunk (HG+SpM). 137 patients had a normal CHA anatomy in which the CHA originated from the celiac axis, and had a suprapancreatic preportal course. In the remaining 13 patients variations in its origin and /or anatomic course were noted.*
Conclusion: *With a clear definition of normal and variant CHA, we were able to perform a systematic analysis of CT images using nomenclature system and summarize the observed variations.*
Keywords: *Coeliac axis, Common hepatic artery , systematic analysis, nomenclature system.*

Introduction

Anatomical variability is noted in the origin of vessels that supply the abdominal organs. A prior knowledge of the extent of variations in vascular anatomy is essential for minimizing serious ischaemic complications in laparoscopic, surgical and vascular interventional radiological procedures. Within the field of interventional radiology, there is an ever-increasing demand for deeper knowledge of the anatomy of the regional vasculature and its variations.

Materials and Methods

The study was conducted at Department of Radiodiagnosis, Government Medical College, Trivandrum. Approval for the study from the Instituitional Research committee and Ethical committee was obtained. The scans of consecutive 100 adult patients who underwent CT scan of abdomen or CT angiogram of abdomen in previous month were taken for the study. Patients with a history of major surgical procedure of abdomen were excluded.

Patients in whom the branches were not well defined on images due to technical reasons - poor patient breath hold causing movement artefacts, or lack of adequate contrast in vessels also were excluded.

CT examination: All studies were done on the multislice (128 slice) CT unit (Siemens) after adequate patient preparation.First nonenhanced images were obtained from the level of diaphragm in a craniocaudal direction. Then oral contrast (iodinated contrast diluted with water in the ratio 1:20) was given to opacify and distend the bowel lumen. The oral contrast volume varied from patient to patient. Then non ionic iodinated contrast media was injected at the rate of 3-4 ml/sec by hand injection through a 18 or 20 gauge plastic canula into the ante cubital vein. Contrast medium volume varied from 70 to 100 ml (delivered at 1.5 ml per kilogram body weight). Hepatic arterial phase images were taken 20 seconds after completion of contrast administration, 20-30 seconds later portal phase imaging was done. Equilibrium phase images were acquired 180 seconds after completion of the contrast administration.

Image interpretation

Continuous images were obtained with slice thickness of 0.6 mm. The images were analysed at GE AW workstation. Coronal and sagittal reconstruction images were also studied.

The pattern of the aortic origin of the coeliac and superior mesentericartery was obtained.

After assessing the coeliac axis anatomy, including its origin site, anatomic course and relationship to surrounding structures, the branching patterns and course of the downstream hepatic arteries –specifically, the common hepatic, left and right hepatic arteries and the gastroduodenal artery was studied .

Description

The origin of arteries arising from the aorta are first evaluated.

Then the coeliac axis is described. The name of the arterial trunks or individual arteries arising from the aorta are connected by plus signs in abbreviations.

Normal anatomy refers to hepatogastrosplenic trunk (HSpG). When naming anarterial trunk the term hepato means the CHAs arise from the trunk. Then the type of CHA variation is described. CHA is defined as an arterial trunk containing at least one segmental hepatic artery and the gastroduodenal artery.

To describe the origin site of a variant CHA branches, the name of the origin site abbreviation is simply connected to the name of the vessel from which it arises by a hyphen. When the right hepatic artery arises from the SMA and left hepatic artery arises from the left gastric artery or the gastroduodenal artery arises directly from the SMA, we describe these variations as RH-SM, LH-LG, GD-SM.

The anatomic course is attached to the end of the type of CHA or branch variation with parentheses. When a variant CHA arises from the SMA and passes through the portocaval space, posterior to the portal vein, and superior to the pancreas, it is described as CH-SM (suprapancreatic, retroportal).

Table 1

Abbreviations and their definitions (1)

Abbreviation	Description and Definition
Ao	Aorta
CA	Coeliac axis
CH	Common hepatic artery – an arterial trunk containing at least one segmental hepatic artery and the gastroduodenal artery, regardless of its origin site or anatomic course.
CM trunk	Coeliaco mesenteric trunk
GD	Gastroduodenal artery
GM trunk	Gastromesenteric trunk
GSpM trunk	Gastrosplenomesenteric trunk
HG trunk	Hepatogastric trunk
HGSp trunk	Hepatogastrosplenic trunk, normal coeliac axis
HM trunk	Hepatomesenteric trunk
HSp trunk	Hepatosplenic trunk
HSpM trunk	Hepatosplenomesenteric trunk
LG	Left gastric artery
LH	Left hepatic artery
PH	Proper hepatic artery, which is an arterial trunk before branching into left and right hepatic arteries, regardless of its origin site or anatomic course.
RH	Right hepatic artery
SM	Superior mesenteric artery
SpM trunk	Splenomesenteric trunk
Sp	Splenic artery

Table 2. Types of coeliac axis anatomy.(1)

1. HGS trunk.
2. HSptrunk+LG+SM
3. HM trunk +GSp trunk
4. CM trunk
5. HSpM trunk +LG
6. HM trunk +LG+Sp
7. HGtrunk+SpM trunk
8. CH+LG+Sp+SM
9. CH +GSpM trunk
10. CH+LG+SpM trunk
11. HG trunk+ Sp+ SM
12. HSp trunk+ GM trunk
13. HGM trunk +Sp
14. CH+ GM trunk+ Sp
15. Ambiguous anatomy

Table 3 - Definition of arterial segments

Segment	Description
Celiac axis	Hepatogastrosplenic trunk (HGSp). SMA originating separately from the aorta.
CHA normal anatomy	CHA originates from the CA and has a Suprapancreatic preportal course, the arterial trunk containing at least one segmental hepatic artery and the gastro duodenal artery regardless of its origin site or its anatomic course
Right hepatic artery	the artery supplying the segments of right lobe of liver
Left hepatic artery	the artery supplying the segments of left lobe of liver
Left gastric artery	seen along the lesser curvature ofstomach arising from CA along with CHA and SpA
Splenic artery	artery supplying the spleen entering through the splenic hilum and taking its origin from CA along with LG and CHA
Gastroduodenal artery	arising from the CHA which originates from CA and seen anterior to first part of duodenum.
Ambiguous celiac axis	Congenital absence of CHA or congenital presence of an anastomotic channel connecting the CA and SMA or anastomotic channel connecting the CHA to the CA and the SMA.

Results

Of the 15 coeliac axis anatomy types, we could identify only 2 types. A total of 149 cases had a normal celiac axis anatomy which appeared as a hepatogastrosplenic trunk and SMA originating separately from the aorta. Variant identified was a hepatogastric trunk with splenomesenteric trunk.

137 patients had a normal CHA anatomy in which the CHA originated from the celiac axis, and had a suprapancreatic preportal course. In the remaining 13 patients variations in its origin and /or anatomic course were noted.

137 patients had both normal right and left hepatic artery anatomy, 140 had normal right hepatic artery anatomy and 147 had normal left hepatic artery anatomy'

Variations in either right or left hepatic artery was found in 13 patients, 10 had variant right hepatic artery anatomy while 3 had variant left hepatic artery. Among the 10 with variant right hepatic artery 9 had its origin from superior mesenteric artery while one was seen rising from the aorta. When the right hepatic artery was seen arising from the aorta, gastroduodenal artery was seen as

a branch of the common hepatic artery which supplied the left lobe. When the left hepatic artery was seen arising from the aorta, gastroduodenal artery was seen as a branch of the common hepatic artery which supplied the right lobe.

All 9 patients in whom right hepatic artery had its origin from superior mesenteric artery, the vessel had a supra pancreatic, retroportal course.

Fig 1 HSpG + SM , RH-SM (suprapancreatic, retroportal)

In this case the CHA arising from the coeliac axis is seen coursing through its normal preportal course before giving off the GA and LH. The RH after taking origin from SM artery is seen taking a suprapancreatic retroportal course.

Fig 2 LH –Ao.

The LH is seen arising as a separate branch from the Aorta. The CA and SM are also seen.

Fig 3 - RH –SM

The RH is seen taking origin from SM.

Discussion

The celiac artery (or the celiac trunk) provides vascular supply to the foregut: it supplies blood to the stomach, the liver, the spleen and the part of the esophagus that reaches into the abdomen. It also supplies the superior (or upper) half of the duodenum and the pancreas.

The superior mesenteric artery is the second of the three major anterior branches of the abdominal aorta. It arises anteriorly from the abdominal aorta at the level of the L1 vertebrae, immediately inferior to the origin of the coeliac trunk.

In describing the branches of coeliac axis, the branching pattern with the highest prevalence has been reported as its division pattern into left gastric, common hepatic and splenic arteries. Among the variations of branching pattern the common hepatic artery is the key component of the variant anatomy. The textbook definition of common hepatic artery is the segment of hepatic artery coursing from the coeliac axis to the point where the gastroduodenal artery branches. But the CHA can have a variant origin other than the coeliac axis and take various anatomic courses.

By tracing back from the organ supplied to its course upto abdominal aorta can be a useful method to delineate the various branching patterns of coeliac axis. The artery supplying the right lobe of liver, right hepatic artery, that supplying left lobe is the left hepatic artery, that supplying spleen is the splenic artery.

Left gastric artery is the vessel which is seen along the lesser curvature and which flows from

left to right to anastomose with the right gastric artery, a branch of hepatic artery and that which flows from right to left. The left gastric artery gives off an oesophageal branch to the distal oesophagus. The branches of the left gastric also anastomoses over the fundus with the short gastric arteries. Short gastric branches are the vessels which arise from the terminal part of splenic artery.

Gastroduodenal artery –the artery which mainly supplies the pylorus, proximal duodenum, and the head of the pancreas. It lies in the gastrohepatic omentum and passes behind the first part of duodenum to reach its lower border, where it divides into two terminal branches – the superior pancreatico duodenal and right gastro epiploic artery. Right gastroepiploic supplies the greater curvature of the stomach and pylorus. It is found between the layers of the greater omentum, which it also supplies. Superior pancreaticoduodenal artery divides into an anterior and posterior branch, which supplies the head of the pancreas. The gastroduodenal artery arise from common hepatic artery.

Fifteen types of coeliac axis anatomy including normal celiac axis is theoretically possible. (see table 2)

To describe the results of the systematic analysis of the coeliac axis and common hepatic artery the segments need to be defined. (Table 3)

Conclusion

With a clear definition of normal and variant CHA, we were able to perform a systematic analysis of CT images using descriptive nomenclature system and summarize the observed variations

Limitations

The number of cases studied was not adequate to be able to describe most of the variants in the population. A study with a large number of patients will be useful to verify the usefulness of the nomenclature.

The study was based on the analysis of radiologic images, depiction of fine arterial networks was not possible as was beyond the capability of CT examinations.Variation in segmental arterial branching was not studied. The implications of the classification has not been studied in surgical and interventional procedures.

References

1. Celiac Axis and Common Hepatic Artery Variations in 5002Patients:Systematic Analysis with Spiral CT and DSA (Radiology 2010; 255:278–288).

2. Mane Uddhav Wamanrao, Kulkarni Yashwant Ramakrishna. -Anatomical study of abdominal aorta and its branches for multiple variations. Int J Anat Res 2016;4(2):2320-2327.
   DOI:10.16965/ijar.2016.205

3. Olga Kornafel, Bogusława Baran, Izabela Pawlikowska, Piotr Laszczyński, Maciej Guziński, Marek Sąsiadek Analysis of anatomical variations of the main arteries branching from the abdominal aorta, with 64-detector computed tomography Pol J Radiol, 2010; 75(2): 38-45Singapore Med J 2012; 53(5) : 329

4. Coeliac trunk and its branches: anatomical variationsand clinical implications Prakash1, MBBS, MD, T Rajini, MBBS, MD, V Mokhasi, MBBS, MD, BS Geethanjali, MBBS, MD,PV Sivacharan, MBBS, MD, M Shashirekha, MBBS, MD Singapore Med J 2012; 53(5) : 329

5. CT angiography of the celiac trunk: anatomy, variants andpathologic findings - Nilgün Işıksalan Özbülbül Diagn Interv Radiol 2011; 17:150–157.

Journal Of Medical Science And Clinical Research
IGM Publication
An Official Publication Of IGM Publication

Diffusion weighted (DW) MRI in assessment of renal function - a preliminary study to determine the Apparent Diffusion Coefficient (ADC) values of kidneys with normal function

Author
Dr Bindu R Kumar
Assistant Professor, Department of Radiodiagnosis, Government Medical College, Trivandrum
Email: *bindupai@hotmail.com*

Abstract

Aim: *To determine the ADC values of kidneys in patients with normal serum creatinine values as an initial step to investigate the clinical potential of diffusion-weighted imaging (DWI) in assessing renal function in comparison with serum markers of renal function.*

Materials and Methods: *MR imaging is performed on 1.5 Tesla MR machine (Siemens) Diffusion weighted images are obtained at b values 0, 50. 400 and 800. Using automated ROI delineation methods ADC values are measured in the upper pole, interpolar region and lower pole of both kidneys. The mean ADC values were recorded for each kidney for each patient is recorded. The patients selected for this study had normal values for serum markers of renal function.*

Results: *The ADC value for renal parenchyma varied from $1.697x 10^{-3}mm^2/s$ to $1.948x10^{-3}mm^2/s$ with a mean ADC value of kidneys ranging from $1.730x10^{-3}mm^2/s$ to $1.885x10^{-3}mm^2/s$*

Conclusion: *Diffusion weighted MR imaging of the kidney can be useful imaging modality in the early determination of renal parenchymal disease especially with unilateral dysfunction. ADC values may predict abnormality earlier than serum markers of renal function.*

Keywords: *Renal parenchymal disease, diffusion weighted imaging (DWI), apparent diffusion coefficient (ADC). estimated glomerular filtration rate (eGFR).*

Introduction

The kidney is a particularly interesting organ to study with DW MR imaging techniques because of its high blood flow and water transport functions. The pathologic changes will restrict the free movement of water molecules in the extracellular extravascular space and can cause a decrease in apparent diffusion coefficient (ADC) values. Patients with chronic kidney disease had significantly lower renal ADC values and that there was a negative correlation between the ADC and serum creatinine level in patients with chronic renal failure.[1]

The study aims at determining the ADC values in kidneys at different stages of renal dysfunction and in a normal population. This can be a standard in the early determination of unilateral renal dysfunction even when the serum creatinine levels are normal. The present study is to try to establish the cut off values for ADC in normal functioning kidneys.

Materials & Methods (Methodology)

After obtaining the clearance from the Instituitional Research committee and Instituitional Ethical committee, the study was conducted at Dept. of Radiodiagnosis, Medical College, Trivandrum. Adult patients who undergo magnetic resonance imaging of the abdomen for various clinical reasons and with normal serum markers for renal function were the subjects for the study.

All data including demographic information, clinical, and laboratory findings were obtained from the medical records of the patients.

The serum creatinine levels are obtained by standard laboratory assay. eGFR is calculated using MDRD equation -

MR imaging is performed on 1.5 Tesla MR machine (Siemens). Diffusion weighted images in the axial plane are taken for calculation of ADC .Diffusion weighted images are obtained at b values 0, 50. 400 and 800. Using automated ROI delineation methods for measurement of ADC values, region of interest (ROI) is placed on the renal parenchyma without any preference for cortex or medulla. Three circular ROIs of 1 cm2 are placed-one each in the upper pole, interpolar region and lower pole of both kidneys. The mean ADC values were recorded for each kidney.

Three subjects with normal serum markers of renal function were the subjects for this preliminary study. Their e GFR was calculated using MDRD equation. These patients had a serum creatinine value less than 1, they had no known history of renal parenchymal disease, had normal echogenicity on sonography and eGFR of less than 90 mL/min/1.73 m$^{2.}$

Results

The ADC value of renal parenchyma at various levels varied from $1.697 \times 10^{-3} \text{mm}^2/\text{s}$ to $1.948 \times 10^{-3} \text{mm}^2/\text{s}$. The average ADC value of kidney varied from $1.730 \times 10^{-3} \text{mm}^2/\text{s}$ to $1.885 \times 10^{-3} \text{mm}^2/\text{s}$

Table 1- Measurements of ADC of renal parenchyma

	Upper pole	Interpolar	Lower pole	Mean
Case 1 RK	1.832	1. 870	1. 875	1.859
LK	1.792	1.760	1.744	1.765
Case2 RK	1.759	1.712	1.871	1.781
LK	1.754	1.739	1.697	1.730
Case 3 RK	1.708	1..881	1.749	1.779
LK	1.948	1.889	1.819	1.885

Discussion

Chronic kidney disease (CKD) is a common global health problem and its average incidence is on the rise with the increase in incidence of hypertension and diabetes. Serum creatinine, and estimated glomerular filtration rate (eGFR) are indirect biochemical tests for assessing renal filtration , however they are imperfect and cannot assess unilateral renal function.

Diffusion weighted MRI is an evolving field and its potential is yet to be fully utilised.

DW MRI is a noninvasive modality to characterise tissues based on Brownian motion of water molecules within them. Apparent diffusion coefficient (ADC) is a quantitative parameter calculated from DWI that combine the effects of capillary perfusion and water diffusion .The pathologic changes will restrict the free movement of water molecules in the extracellular extravascular space. This cause a decrease in apparent diffusion coefficient (ADC) values.

Kidney is an organ with high blood flow and water transport functions.Preliminary research has shown that patients with chronic kidney disease had significantly lower renal ADC values .There was a negative correlation between the ADC and serum creatinine level in patients with chronic renal failure.

eGFR is calculated using Modification of Diet in Renal diseases (MDRD) equation -

$$eGFR = 186 \times (Creat / 88.4)^{-1.154} \times (Age)^{-0.203} \times (0.742 \text{ if female})$$

Chronic kidney disease (CKD) is graded into five stages based on disease severity, according to the K/DOQI (kidney disease outcomes quality initiative) CKD classification.

Stage 1: eGFR; $\geq$90 mL/min/1.73 m^2 (kidney damage with normal or increased eGFR).

Stage 2: eGFR; 60–89 mL/min/1.73 m^2 (kidney damage with a mild reduction in eGFR).

Stage 3: eGFR; 30–59 mL/min/1.73 m^2 (moderate reduction in eGFR).

Stage 4: eGFR; 15–29 mL/min/1.73 m^2 (severe reduction in eGFR).

Stage 5: eGFR; < 15 mL/min/1.73 m^2 (kidney failure).

Various studies indicate there is a relation between the ADC values and eGFR.

In a study published in the European Journal of Radiology [1] on 110 patients with CKD , ADC values ranged between 0.839 and 1.508 (x 10^{-3} mm^2/s) In a study published in the Indian Journal of Radiology and Imaging Goyal, et al.[2] reported that the mean ADC values of different stages of CKD were significantly different from each other and showed a decreasing trend with increasing stage using *b*-values ranging between 0 and 500 s/mm^2.

Normal renal function involves multiple processes of water transport, while worsening renal function (reduction in GFR) should lead to a decrease in water reabsorption, i.e. a lower rate of water transfer across interstitial space. This would potentially reduce diffusion. In addition, fibrosis formed in the process of chronic renal dysfunction may also restrict water diffusion.

Conclusion

The present study in normally functioning kidneys showed the ADC value of kidneys to range from 1.730x10^{-3}mm^2/s to 1.885x10^{-3}mm^2/s. A decrease in renal function due to fibrosis will lower the ADC values and there could be a correlation between the various stages of renal parenchymal disease and decreasing ADC values.

References

1. The relationship of ADC values of renal parenchyma with CKD stage and serum creatinine levelsdoi: 10.1016/j.ejro.2015.10.002
2. Diffusion-weighted MRI in assessment of renal dysfunction. Indian J. Radiol. Imaging. 2012;22:155–159.
3. Diffusion-weighted MR Imaging of Kidneys in Healthy Volunteers and Patients with Parenchymal Diseases: Initial Experience – Radiology doi.org/10.1148/radiol.2353040554
4. Diffusion-weighted MRI in assessment of renal dysfunction, Indian J Radiol Imaging. 2012 Jul-Sep; 22(3): 155–159. doi: 10.4103/0971-3026.107169,

Journal Of Medical Science And Clinical Research

IGM Publication   An Official Publication Of IGM Publication

Research Article
Tuberculous Spondylodiscitis – Characteristic Features with MR Imaging

Author
Dr Bindu R Kumar
Assistant Professor, Department of Radiodiagnosis, Government Medical College, Paripally, Kollam
Corresponding Author
Dr Bindu R Kumar

Abstract
Aim: *To determine the main MRI characteristic features of tuberculous lesions of the spine in clinically confirmed cases of tuberculous spondylodiscitis*
Materials and Methods: *MRI images of patients with clinically proven Tuberculous spondylodiscits was assessed and the findings assessed to determine the characteristic features.*
Result: *The most commonly involved part was the thoracic spine. Para vertebral abscesses with destruction of the vertebrae and discs were seen in seven out of eight patients.*
Conclusion: *The study matches with the features described in literature.*

Introduction
Tuberculosis of the spine is a potentially life-threatening infection because it can produce neurological complications. It is one of the most common world-wide causes of a kyphotic spinal deformity.

Aim of the study
To determine the main MRI characteristic features of tuberculous lesions of the spine in clinically confirmed cases of tuberculous spondylodiscitis.

Materials and Methods
It is a retrospective study on 8 patients diagnosed as having tuberculous spondylodiscitis either clinically, histopathology and/or imaging and treated with anti tuberculous treatment for 12 months. MR scan taken at the time of diagnosis and at the end of 12 months of antituberculous treatment formed the main basis of the study. The various characteristics that define the lesion and its complications were studied using MRI scan. These patients had attended the neurology clinic of Government Medical College, Trivandrum with complaints of back pain/neck pain with or without significant neurological deficit.

MRI scan was performed on 1.5 Tesla MR scanner, Siemens, Germany installed in the Department of Radiodiagnosis, Medical college, Trivandrum from July 2019 to December 2019. Basic sequences T1w, T2w, and post contrast images formed part of the study taken for diagnostic purpose. This study is done as part of a larger study on CNS Tuberculosis.

The characteristics that were analysed were – 1.level of involvement 2. Number of vertebrae involved 3. Loss of vertebral height 4. Paravertebral abscess 5. Signal intensities on T1w

and T2w images 6. Wall of lesion 7. Contrast enhancement of the lesion 8. Cord compression involvement of cord compression.

Findings

The findings of the study are tabulated in Tables 1 and 2

Table 1 Morphological characteristics of the lesion

	Patient 1	2	3	4	5	6	7	8
Level of involve ment	Thoracic T6-T12	Thoracic T2-T4	Thoraci T9-T10	Lumbar L1-L3	Thoracic T9-T12	Thoracic T3-T4	C5,T7, L5	L5-S1
Number of vertebrae	6	3	2	3	4	2	3	2
Loss of vertebral height	Nil	More than 75%	50%	10%	More than 75%	nil	10%	nil
Para vertebral abscess present	Yes	No	Yes	yes	Yes	yes	nil	yes

Figure 1 - T2w image showing extensive involvement of lower thoracic vertebrae. There is destruction of the anterior and posterior cortices of vertebral bodies and compression of the cord .
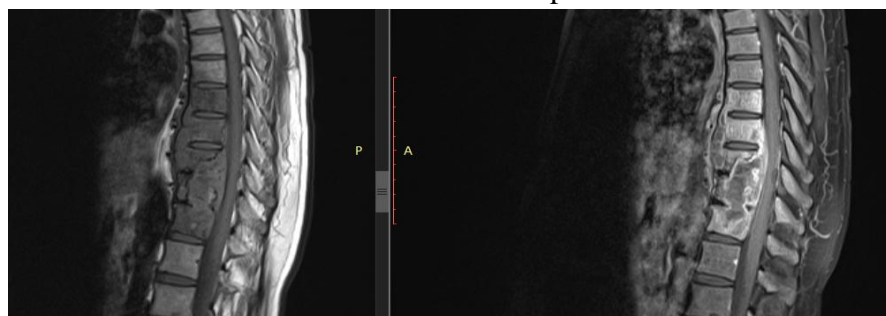
Figure 2 – T1w and post contrast sagittal images. The lesion on T1w is hypointense, post contrast images shows extensive intraosseous abscess – non enhancing area with enhancing wall at the site of thoracic vertebral bodies

Table 2: MR imaging characteristics of the lesion

At time of diagnosis	Patient 1	2	3	4	5	6	7	8
Signal intensity on T1w (compared to normal bone marrow)	hypo	hypo	hypo	hypo	hypo	hypo	hypo	hypo
Signal intensity on T2w (compared to normal bone marrow)	Heterogeneously hyper	hyper	hyper	hyper	hyper	hyper	hyper	hyper
Wall of lesion	Well defined	Well defined	Ill defined partially	Well defined	Well defined	Ill defined	Well defined	Well defined
Contrast enhancement-predominant	Hetero genous Hypo enhan cing	Homo genous Hypo enhan cing	Hetero genous Hyper enhan cing	Heteroge nous Hyper enhan cing	Homo genous Hypo enhan cing	Homo genous Hyper enhan cing	Homoge nous Hyper enhan cing	Hetero genous Hypo enhan cing
Cord compression	Present	present	present	nil	present	nil	nil	Nil

Discussion

MR imaging is considered superior for accurately defining the epidural extension of the disease and neural structure involvement.[1] Loss of vertebral body cortical definition and the presence of a paraspinal mass with thick irregular rim enhancement favour tubercular over bacterial spondylodiscitis Because of its superior ability to detect marrow changes before any bony destruction, MR imaging plays an important role in early diagnosis even in patients with normal radiographs. In majority of cases, tubercular spondylitis appears hyperintense on T2-weighted images and hypointense on T1-weighted images with contrast enhancement indicating marrow edema in the infected area. An important imaging feature that characterizes tuberculous infection compared to bacterial infection is sparing of the intervertebral disc in the early stage of infection. Conversely, early spread to discs with loss of disc height and disc herniation favor bacterial infection .Other characteristic involvement of the anterior vertebral body corner, subligamentous spread, multiple vertebral bodies, extensive paraspinal abscess formation, abscess calcification, and vertebral destruction differentiates tubercular from bacterial spondylodiscitis.

The patients in the study presented to the neurology department either with severe back pain and neurological deficit, and are clinically proved cases of spondylodiscitis. The most commonly involved part is lower thoracic spine. One patient had involvement of cervical spine and another had lesion at L5-S1. One patient had lesions at multiple levels with no intervertebral disc involvement. 5 out of 8 patients had loss of vertebral height and cord compression accounting for the neurological deficits. Paravertebral abscesses were seen in all except one where there was no intervertebral disc involvement. The paravertebral abscess were largest in the L5-S1 patient with extensive involvement of the pelvic wall and subcutaneous compartment.

The lesions were homogenously hypointense on T1w images, heterogeneously hyperintense on T2w. The lesion showed peripheral enhancement with intraosseous and soft tissue paravertebral abscesses.

None of the patients underwent therapeutic intervention. The abscesses resolved completely. The main clinical problem was the neurological deficit caused due to cord compression due to loss of vertebral height and gibbus deformity which was seen as sequelae to established cases of spondylodiscits.

References

1. Kumar Y, Gupta N, Chhabra A, Fukuda T, Soni N, Hayashi D. Magnetic resonance imaging of bacterial and tuberculous spondylodiscitis with associated complications and non-infectious spinal pathology mimicking infections: a pictorial review. BMC Musculoskelet Disord. 2017 Jun 5;18(1):244. doi: 10.1186/s12891-017-1608-z. PMID: 28583099; PMCID: PMC5460517.

2. Procopie I, Popescu EL, Pleşea RM, Dorobanţu M, Mureşan RF, Lupaşcu-Ursulescu CV, Pleşea IE, Anuşca DN. Clinical-Morphological Aspects in Spinal Tuberculosis. Curr Health Sci J. 2018 Jul-Sep;44(3):250-260. doi: 10.12865/CHSJ.44.03.08. Epub 2018 Jul 15. PMID: 30647945; PMCID: PMC6311224.

Journal Of Medical Science And Clinical Research
IGM Publication   An Official Publication Of IGM Publication

Research Article

Post contrast T2 -FLAIR sequence - can it be a predictor of disease activity in tuberculomas of brain – findings from a preliminary study

Author
Dr Bindu R Kumar
Assistant Professor, Department of Radiodiagnosis, Government Medical College, Paripally, Kollam
Corresponding Author
Dr Bindu R Kumar

Abstract
Aim: *To assess the use of pre and post contrast T2 FLAIR images in brain scans in CNS tuberculomas as a predictor of disease activity.*
Materials and Methods: *T2 FLAIR pre and post contrast images and T1w post contrast images of clinically proven cases of tuberculomas in brain in various stages of antituberculous treatment were taken. The images were reviewed to particularly study the intensity and enhancement of the lesions.*
Result: *There was a clear difference in the enhancement of the rim of the tuberculoma in patients in different stages of antituberculosis treatment on T2 FLAIR images.*
Conclusion: *The results of the study are from a small sample. Our study was based on only six patients and hence is only a preliminary study. A study with a larger sample size is needed.*
Keywords: *Tuberculoma, T2 FLAIR, pre and post contrast images.*

Introduction

T2-FLAIR stands for ***T2-weighted-Fluid-Attenuated Inversion Recovery***. Originally just called "FLAIR", this technique was developed in the early 1990's by the Hammersmith research team led by Graeme Bydder, Joseph Hajnal, and Ian Young. Their original sequences used TI values of 2000-2500 to null signal from CSF, coupled with very long TRs (8000) and TEs (140) to create strong T2-weighting.[3]

Fluid-attenuated inversion recovery (FLAIR) is a special inversion recovery pulse sequence with a long repetition time (TR) and echo time (TE), and an inversion time (TI) that effectively nulls signals from the cerebrospinal fluid (CSF) The T2-FLAIR technique repeatedly proved itself by revealing a wide range of lesions, including cortical, periventricular, and meningeal diseases that were difficult to see on conventional images.[1]

Due to the long TI (2000 -2500ms) in FLAIR sequences, the FLAIR images also show mild T1w effects. Some lesions may not be conspicuous with low doses of Gd on T1w post contrast sequences these may be better appreciated on T2 w FLAIR sequences.

Aim

The aim of the study is to assess the use of pre and post contrast FLAIR images in brain scans in CNS tuberculomas. Although T1w imaging is typically used in contrast imaging, our study was also to compare the enhancement of lesions on post contrast T2 FLAIR and T1w post contrast images.

Materials and Methods

The subjects were six clinically or microbiologically proven cases of CNS tuberculosis in different stages of treatment who underwent MR imaging as part of a larger study on CNS tuberculosis which was done in Government Medical College, Trivandrum after obtaining ethical committee clearance. In all cases basic pre contrast sequences included FLAIR sequence of brain. MR imaging was done on 1.5 Tesla scanner (Avanto; Siemens Medical Solution, Germany).After the basic sequences, contrast agent (gadobutrol [Gadovist]; Bayer Healthcare, Berlin, Germany) was administered as per the protocol at the standard dose of 0.1 mmol/kg of body weight. In our institution, contrast enhanced T1weighted images is the sequence routinely used in lesion detection at brain MRI. Routine post contrast multiplanar T1w images were taken as usual. Immediately after that axial FLAIR imaging was done.

Images of pre contrast FLAIR and post contrast FLAIR were compared to see the areas of altered signal intensities and contrast enhancement. Post contrast FLAIR images were compared with post contrast multi planar T1w images for assessment of lesion enhancement.

Results

Of the six cases, four patients had completed twelve months of anti tuberculosis treatment. One patient had completed four months of treatment and another patient was a case of relapse.

Two patients who had completed twelve months of antituberculous treatment had complete resolution of lesions with no enhancing lesions on post contrast FLAIR or post contrast T1w images.

The other two patients who had completed 12 months of ATT had multiple lesions in parenchyma which were hypointense on T2 FLAIR and of size less than 1 cm. On post contrast scans these lesions showed well defined ring enhancement on T1w images but no enhancement of the lesion was seen on post contrast FLAIR images. (Fig 1)

One patient who had disseminated miliary tubercles and tuberculous meningitis at the time of diagnosis showed multiple hypointense foci on FLAIR images in the parenchyma adjacent to bilateral Sylvian fissures. This patient had very tiny foci of hyperintensity scattered in the cerebral cortex seen only on FLAIR images with no visible enhancement on post contrast FLAIR or post contrast T1w images. (Fig 2) This patient was asymptomatic at the time of scan. These tiny foci of cortical hyperintensity on T2 FLAIR could represent gliosis or burned out tuberculous foci. We could not prove it by histopathology.

The MRI scan of the patient who had completed four months of treatment and had shown clinical improvement showed multiple lesions in parenchyma hypointense on T2 FLAIR images. Some of these lesions on post contrast T2 FLAIR images showed ring enhancement as well as seen on T1w images. Other lesions showed enhancement only on T1w post contrast images. (Fig 3)

The MRI of the patient who presented with relapse showed ring enhancement of the lesions on post contrast T1w and T2 FLAIR as well. Such a ring enhancement of the lesions was seen in the post contrast T1w and T2 FLAIR images. (Fig 4)
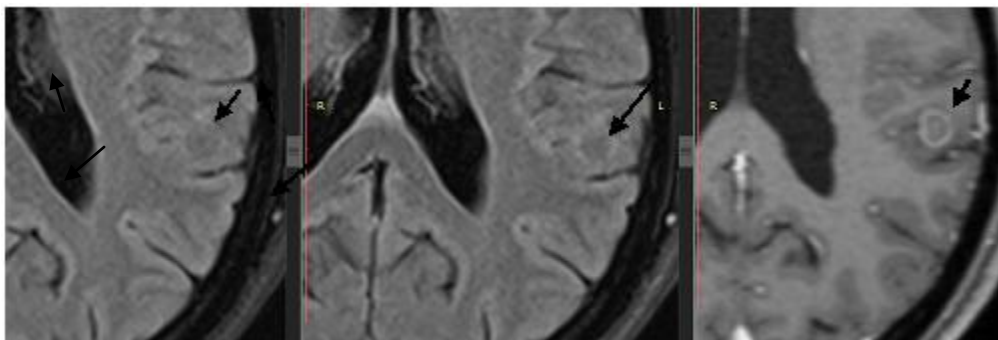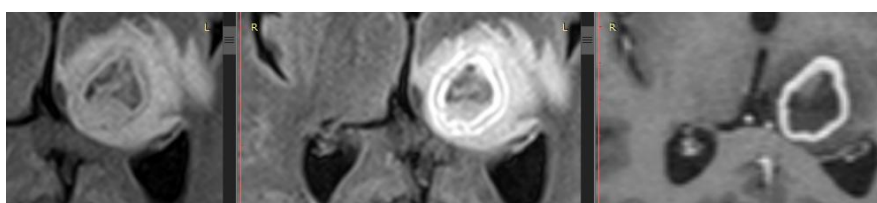
Fig 1 Pre contrast FLAIR, post contrast FLAIR and post contrast T1w axial images.

A hypointense lesion –tuberculoma is seen on precontrast T2 FLAIR, with very minimal peripheral enhancement at the rim on post contrast FLAIR images. On T1w post contrast images the lesion is seen as well defined rim enhancing lesion .This patient had completed 12 months of antituberculosis treatment and was asymptomatic.
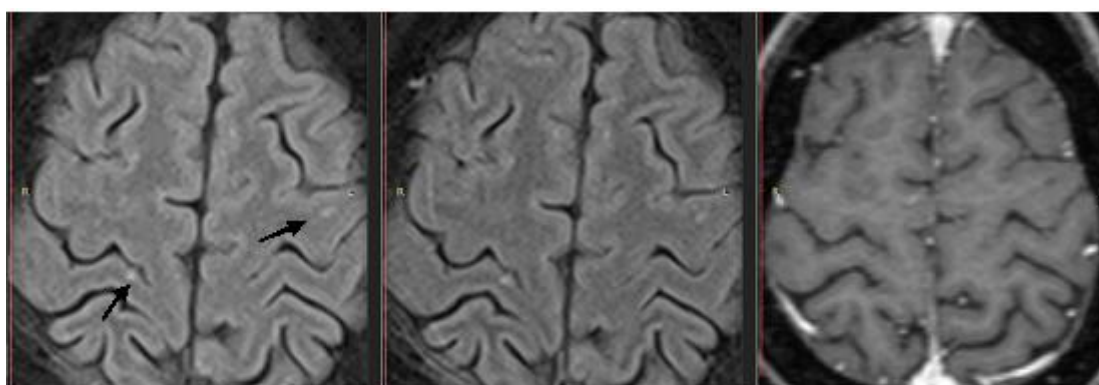
Fig 2. Pre contrast T2 FLAIR, post contrast T2 FLAIR and Post contrast T1w axial images. Tiny hyperintensities are seen in grey matter and subcortical white matter which do not show enhancement on post contrast images.

Fig 3: Pre contrast T2FLAIR ,post contrast T2 FLAIR and post contrast T1w axial images On post contrast T2 FLAIR , the rim of the lesion is seen to enhance with a double ring .On post contrast T1w FLAIR, well defined enhancement of the rim is seen. This was a a biopsy proven case of CNS tuberculoma with relapse.
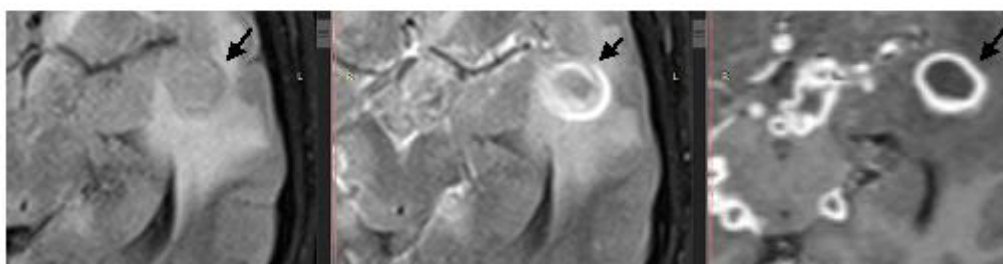
Fig 4 – Pre contrast   T2 FLAIR, Post contrast T2 FLAIR and post contrast T1w images: Rim enhancement is seen on both T2 FLAIR and T1w post contrast images this patient is on ATT for past 4 months. Clinically has improved.

Discussion

Contrast enhancement (CE) in the CNS is the result of a combination of 3 processes: for intra-axial brain lesions, the blood brain barrier (BBB) must be disrupted for Gd to enter the extracellular space; for extra-axial lesions, enhancement is observed in lesions with relatively high vascularity; and for leptomeningeal regions, contrast leakage occurs from vessels into the CSF. Understanding the normally enhancing structures on CE - FLAIR imaging from review of literature can provide a reference point for routine interpretation[2]. In previous reports in children, the choroid plexus, pituitary infundibulum, and cavernous sinus showed relatively intense enhancement,. and the pituitary gland, pineal gland and nasal mucosa/ turbinates are mildly enhanced. However, unlike CE-T1WI, FLAIR enhancement in the pineal gland, pituitary gland and nasal mucosa/turbinates can be difficult to recognize, or show subtle changes due to intrinsic T2 prolongation on pre-contrast FLAIR images.

On CE-FLAIR imaging, most blood vessels do not show enhancement, probably due to a T2 effect of the FLAIR sequence. Additionally, the degree of enhancement in normal intracranial structures on CE-FLAIR imaging appears less intense than that on CE-T1WI, probably because of a mild T1 effect of FLAIR imaging.

Among our patients contrast enhancement of lesions on FLAIR images and T1w multiplanar images were not similar. In patients who had completed 12 months of treatment and who were clinically asymptomatic following antituberculous treatment the lesions on FLAIR images did not show ring enhancement of lesions. But these lesions showed smooth ring enhancement on T1w images.

Conclusion

A well defined ring enhancement of lesions on post contrast FLAIR images only in patients who are clinically symptomatic and with less than six months of ATT raises the possibility of making it a marker sequence to assess activity of tuberculomas. Our study was based on only six patients and hence is only a preliminary study. A study with a larger sample size is needed.

References

1. Importance of Contrast-Enhanced Fluid-Attenuated Inversion Recovery Magnetic Resonance Imaging in Various Intracranial Pathologic Conditions Korean J Radiol 2016;17(1):127-141.
2. Post-contrast FLAIR MR Imaging of the Brain in Children: Normal and Abnormal Intracranial Enhancement Pediatr Radiol. 2003 Dec;33(12):843-9.doi: 10.1007/s00247-003-1057-8. Epub 2003 Oct 10.
3. Normal Findings on Brain Fluid-Attenuated Inversion Recovery MR Images at 3T M. Neema Z.D. Guss J.M. Stankiewicz A. Arora B.C. Healy R. Bakshi AJNR Am J Neuroradiol 30:911–16 , May 2009 , www.ajnr.org